25th ABCM International Congress of Mechanical Engineering
October 20-25, 2019, Uberlândia, MG, Brazil

EFFECT OF LOAD RATIO ON FATIGUE CRACK GROWTH IN THE NEAR-THRESHOLD REGIME IN STEELS FOR AUTOMOTIVE APPLICATIONS USING A COMBINED CRACK CLOSURE AND DRIVING FORCE APPROACH

Tainan Ferreira Muniz
Leonardo Barbosa Godefroid
Universidade Federal de Ouro Preto, Ouro Preto, MG, Brazil
tainanfmuniz@yahoo.com.br; leonardo@ufop.edu.br

Jefferson José Vilela
CDTN-CNEN, Belo Horizonte, MG, Brazil
jjv@cdtn.br

Fabiano Alcântara Machado
MaxionWheels, Limeira, SP, Brazil
fabiano.machado@maxionwheels.com

Abstract. *The research consisted in the study of fatigue crack growth resistance of one HSLA steel and three AHSS steels, all materials for automotive applications, and the effect of R load ratio on these materials. The results were used to check a single model that could predict the material behavior in the near threshold ΔK_{th} region. For this, the methodology proposed recently by Zhu, Xuan and Tu (2013, 2015) was used to combine two approaches currently adopted in this context: by crack closure and two-parameters driving force. The microstructure of the steels was characterized by optical microscopy and scanning electron microscopy. Basic mechanical tensile and hardness tests were performed. C(T) test specimens with 3mm thick were used for the fatigue tests at room temperature and at a frequency of 35Hz, with a load ratio of 0.03, 0.1, 0.4, 0.5 and 0.7. The traditional effect of fatigue strength loss with increasing load ratio was verified. The application of the mentioned model was evaluated, from the comparison between the values for the experimental and predicted threshold ΔK_{th}, showing that the methodology developed needs improvements to reduce some verified errors.*

Keywords: *Fatigue crack growth, Load ratio, Crack closure, Driving force parameters, Steels for automotive industry.*

1. INTRODUCTION

Since the concepts of fracture mechanics were applied to characterize the fatigue phenomenon in the 1960s, the effect of load ratio (or stress ratio), R, which is defined as the ratio of minimum to maximum load ($R = P_{min}/P_{max}$), on fatigue crack growth (FCG) has been investigated by several researchers. The FCG are found to be faster at higher R, and more sensitive to R when approaching the fatigue threshold, ΔK_{th}. As a result, great attention has been paid to the influence of R on FCG behavior in the near-threshold regime in several materials, for example: low alloy steels (Ritchie, 1979; Liaw *et al*., 1983), pearlitic steels (El-Shabasy and Lewandowski, 2004; Godefroid *et al*., 2019), aluminum alloys (Al-Rubaie *et al*., 2008; Jones *et al*., 2012), titanium alloys (Dubey *et al*., 1997; Boyce and Ritchie, 2001) and nickel alloys (Roy *et al*., 2010; Zhihong *et al*., 2011).

Two main approaches have been currently used to characterize the FCG dependence of materials with the R ratio. On the one hand, the concept of crack closure proposed by Elber (1971) is widely used to explain the influence of R on the fatigue behavior and has generated several adaptations to describe the FCG over the past few decades. On the other hand, Vasudevan and co-workers (1994) proposed a two-parameter driving force approach where ΔK (stress intensity factor range, $K_{max} - K_{min}$) and K_{max} (maximum applied stress intensity factor) are both required to FCG, without invoking crack closure. However, application of these two approaches independently to R-effect in the near-threshold fatigue regime is observed to be either shortage of accuracy or full of uncertainties, as a result of the complexities and difficulties in both experimental measurement and modeling key parameters in the case of the load-shedding procedure. One possible solution to this issue is to take both the two approaches into account by using a suitable merging technique.

Recently, Zhu and co-authors (2013, 2015) investigated the R-effect on FCG, combined the crack closure concept and the two-parameters approach method. They considered a new crack opening equation, without involving crack closure measurement, and an equation relating the crack growth rate da/dN to the driving force ΔK in the near-threshold regime

(ΔK_{th}), on the basis of several values for the *R* ratio. This new model assumes the existence of the crack closure, however only influencing the FCG below a certain value for the *R*. A general FCG equation in the form of the traditional and well known Paris equation, $da/dN = C(A(R)\Delta K^{B(R)})^m$, was put forward for the near-threshold FCG, which was reasonably used to predict *R* dependence of FCG curve and fatigue threshold, with the *C* and *m* constants valid only for this region. This FCG equation was further validated using FCG data in the open literatures and believed to be eligible and suitable to predict fatigue thresholds in a variety of Cr–Mo–V steels.

The methodology proposed by Zhu and co-authors (2013, 2015) requires an FCG test with a relatively high R value (reference value), when there is no influence of crack closure. The generated curve *da/dN versus* ΔK in the threshold region gives reference values for the driving force ΔK_{ref}. From these reference data, values of $(da/dN)_R$ and $(\Delta K)_R$ are obtained for any value of R, using Eq. (1) and Eq. (2), respectively, and the material-specific analytical equations A and B including R as a variable, provided by Eq. (3) and (4)

$$\left(\frac{da}{dN}\right)_R = C\left(\frac{1}{A(R)}\cdot\left(\Delta K_{(ref)}^{(1-B(R))}\right)\right)^m \quad (1)$$

$$(\Delta K)_R = \frac{1}{A(R)}\cdot\Delta K_{ref}^{(1-B(R))} \quad (2)$$

$$A(R) = aR^2 + bR + c \quad (3)$$

$$B(R) = dR + e \quad (4)$$

In the present research, the fatigue crack growth resistance of one HSLA steel and three AHSS steels, all materials for automotive applications, and the effect of R load ratio on these materials were evaluated. The results were considered to check the methodology proposed by Zhu and co-authors (2013, 2015). Values of the load ratio R between 0.03 and 0.7 were used to generate *da/dN x* ΔK curves with emphasis on the crack growth threshold region (ΔK_{th}).

2. MATERIALS AND METODOLOGY

Four low carbon steels in a hot rolled condition and manufactured for automotive applications were studied. The materials were identified as S1 (HSLA ferrite-pearlite steel), S2 (AHSS ferrite-pearlite-bainite Nb steel), S3 (AHSS ferrite-bainite Mn-Nb steel) and S4 (AHSS ferrite-martensite Mn-Cr steel). Fig. 1 presents these studied steels in the form of the called "global formability diagram", that is used to characterize the range of properties available from today's AHSS automotive grades steels (Keeler and Kimchi, 2017).

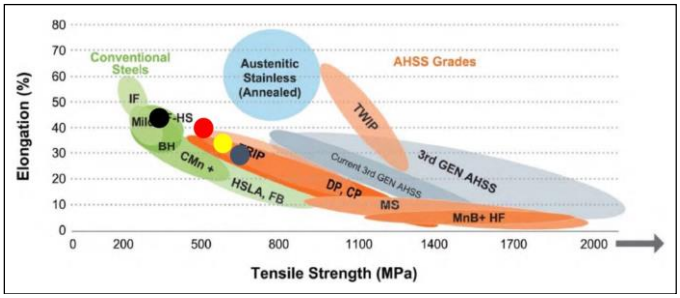

Figure 1. Global formability diagram, adapted from Keeler and Kimchi, 2017.
Black circle = S1; Red circle = S2; Yellow circle = S3; Blue circle = S4.

The samples used for microstructural examination were cut, ground, polished and etched with a special solution developed to reveal microconstituents of high strength steels (De *et al*., 2003). The samples were examined using a LEICA optical microscope (LOM) and a TESCAN VEGA3 scanning electron microscope (SEM). Micrographs are shown in Fig. 2 and Fig. 3. The corresponding grain size and volume fraction of the phases of each steel is shown in Tab. 1.

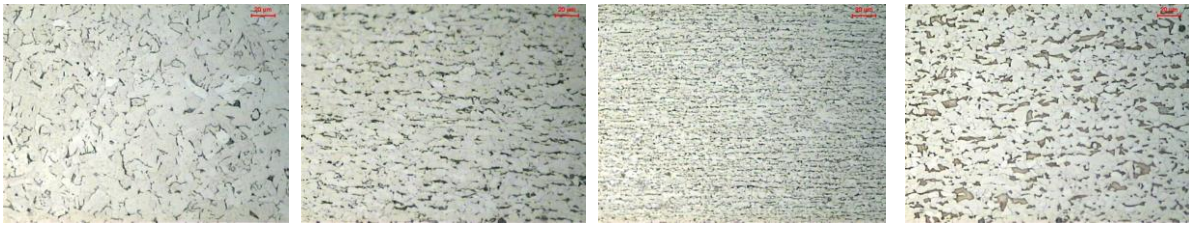

(a) S1 steel (b) S2 steel (c) S3 steel (d) S4 steel
Figure 2. Microscopical analysis of the studied steels. LOM. Original magnification = 500X.

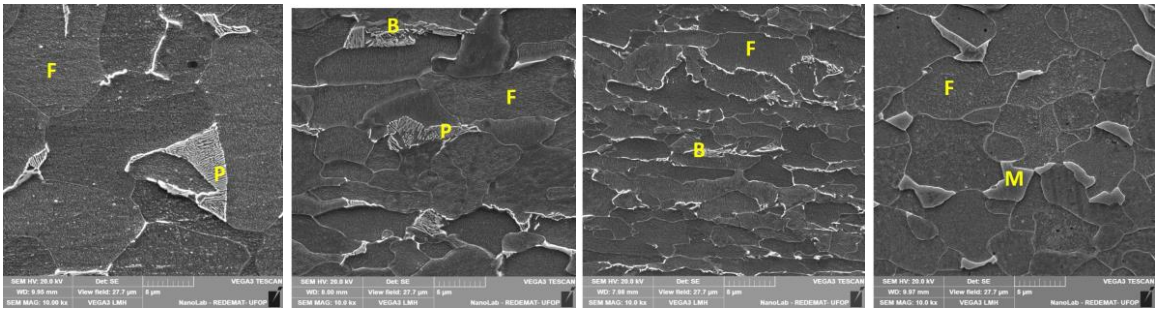

(a) S1 steel (b) S2 steel (c) S3 steel (d) S4 steel

Figure 3. Micrograph of steels. SEM. Original magnification = 10000X.
F = ferrite; P = pearlite; B = bainite; M = martensite.

Table 1. Grain size and phase/constituents volume fraction.

Steel	ASTM grain size	FVF (%)	PVF (%)	BVF (%)	MVF (%)
S1	11 ± 0.4	92.7 ± 0.5	7.3 ± 0.5	-	-
S2	13 ± 0.3	92.6 ± 2.6	4.5 ± 2.0	3.0 ± 1.0	-
S3	14 ± 0.7	96.9 ± 0.6	-	8.0 ± 0.5	-
S4	13 ± 0.3	94.0 ± 2.8	-	-	14.1 ± 1.7

FVF = ferrite volume fraction; PVF = pearlite volume fraction;
BVF = bainite volume fraction; MVF = martensite volume fraction.

Table 2 shows tensile properties of the steels obtained on a 100kN 5882 Instron electro-mechanical system interfaced to a computer for machine control and data acquisition. This table also shows hardness values. The tensile strength, strain-hardening coefficient and strain to fracture are in accordance with the classification for HSLA and AHSS steels used in the automotive industry (Keeler and Kimchi, 2017; Dasarathy and Goodwin, 1990). It can be seen an inverse relation between the mechanical strength and the ductility of the steels, due the presence of different phases/constituents, elements in solid solution, precipitates and ferritic grain size (Krauss, 2005).

Table 2. Tensile and hardness properties of the steels.

Steel	YS (MPa)	UTS (MPa)	DEF (%)	AR (%)	n	HV
S1	265 ± 35	350 ± 34	44 ± 2	68 ± 2	0.18	124 ± 2,4
S2	423 ± 2	493 ± 5	42 ± 3	63 ± 3	0.20	180 ± 13,7
S3	493 ± 9	548 ± 6	35 ± 2	59 ± 4	0.15	188 ± 3,4
S4	402 ± 7	636 ± 8	31 ± 1	52 ± 2	0.21	203 ± 2,1

YS: Yield Strength; UTS: Ultimate Tensile Strength; DEF: Strain for fracture; AR: area reduction;
n: strain-hardening coefficient; HV: Vickers Hardness.

All the fatigue crack growth tests were performed on a 100kN 8802 Instron servo-hydraulic materials testing system interfaced to a computer for machine control and data acquisition, at room temperature in atmospheric air. The tests were conducted under a sinusoidal waveform with a frequency of 35Hz, in accordance with the recommendations of ASTM E647 Standard (2016). Compact tension C(T) specimens oriented in T-L direction were considered for each steel, with 3mm thickness, 50mm width (W) and a fatigue pre-crack length of 3mm to have an initial crack size (a) to width ratio (a/W) of 0.26. Crack opening displacement (COD) measurements were performed using a COD extensometer and crack size evaluation was performed using the compliance method. Crack size curves in function of the number of cycles have been obtained, and transformed to crack growth rate curves (da/dN) as a function of cyclic stress intensity factor (ΔK). Five R-ratio are considered: R = 0.03, 0.1, 0.4, 0.5 and 0.7. The fatigue threshold value ΔK_{th} was defined as the stress intensity factor range at which the fatigue crack growth rate decreased to below $1x10^{-7}$ mm/cycle. This value was estimated by a K-decreasing procedure (load-shedding process), limiting the normalized K-gradient, $C = (1/K).(dK/da)$ to $-0.08mm^{-1}$. ΔK_{th} was obtained from the best-fit straight line from a linear regression of *log da/dN versus log* ΔK between growth rates of 10^{-6} and 10^{-7} mm/cycle.

The critical value of R when crack closure tends to be absent (R_c) was identified using the deviation of linearity of the load x COD curves for the all considered R values. In order to apply the model proposed by Zhu and co-authors (2015), the value of R = 0.7 was chosen as reference where no crack closing occurred. For six specific da/dN values, graphs were plotted between $ln\Delta K$ and $(2R/(1-R))$ for different R and the slope of each line (α) was taken. When R is less than R_c, α is called α_1, otherwise α is equal to α_2. For each test performed with different R, the Paris equation was applied to the region of ΔK_{th} with the correction for ΔK according to Eq. 5 and the constants C_0 and m_0 were obtained. From the parameters C_0, m_0, α_1 and α_2, the crack closure coefficient $U_{(R)}$ is obtained by Eq. 6 and later simplified in Eq. 7, using Eq. 3 and Eq. 4. With this information it can use Eq. 1 – Eq. 4, to predict the fatigue crack growth in the near-threshold regime for different values of R.

$$\Delta K_0 = \Delta K_R \, exp^{\left(\alpha \frac{2R}{1-R}\right)} \tag{5}$$

$$U_{(R)} = \frac{\left(\frac{C_{0(R)}}{C_{0(ref)}}\right)^{1/m_{0(R)}}}{\exp\left(18\alpha_2 - \alpha\frac{2R}{(1-R)}\right)} \cdot (\Delta K_{0(ref)})^{\,1-(m_{0(ref)}/m_{0(R)})} \tag{6}$$

$$U_{(R)} = A(R).\Delta K_{0.7}^{B(R)} \tag{7}$$

3. RESULTS AND DISCUSSION

The sigmoidal *da/dN versus ΔK* curves for the four steels, with *R* = 0.1, are presented in Fig. 4. It is possible to see the three different regions of FCG commonly found in metals. When comparing the fatigue behavior of the steels, it is observed that they have similar behavior in the linear Region II, since this region is less sensitive to chemical composition and microstructure. In region I and region III, there is a significant different behavior among the steels, since the FCG in these regions is strongly influenced by the chemical composition and the microstructure of the material (Minakawa *et al*., 1982; Godefroid *et al*., 2011; Dutta *et al*., 1984; Ramage *et al*., 1987; Sarwar and Priestner, 1999; Sun *at al*., 1995). The S3 presented the highest value of ΔK_{th}, having, then, the best fatigue performance among the materials, followed by S4 steel. The best performance of AHSS steels is reported in the literature (Gritti et al., 2014; Gutz *et al*., 2010) as a consequence of the presence of the dual-phase microstructure, i.e., bainite or martensite in a ferritic matrix. In this case, the FCG in the ferrite will create tortuosity and bifurcation when the crack encounters the hardest phase, the driving force decreases and the FCG rate decreases.

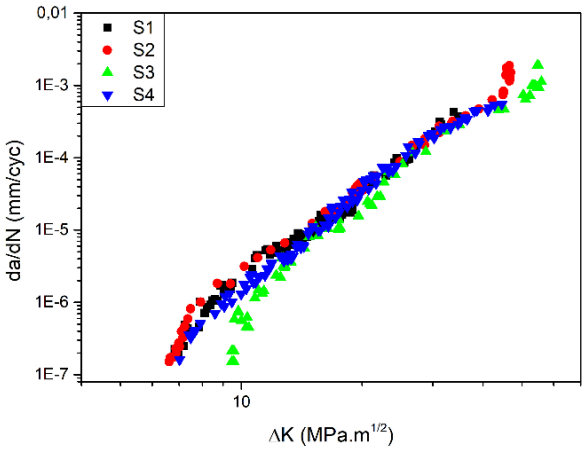

Figure 4. Sigmoidal curves *da/dN versus ΔK* with *R* = 0.1 for all studied steels.

The SEM images taken from the fracture surfaces of fatigue tests are showed in Fig. 5 and Fig. 6 for *R* = 0.1. For all steels the fracture surface presented at the near-threshold region (Fig. 5) a predominant transgranular fracture mode, with the "hill-and-valley" type appearance and shear facets, with an associated zig-zag path primarily through the ferrite. Such fractures show high linear roughness and high crack deflection angles. At higher growth rates, characteristics of region II (Fig. 6), fracture surfaces remain transgranular, but with evidence of striations. These fracture mechanisms did not change with the change in the value of *R*.

The deleterious effect of increased *R* ratio on the ΔK_{th} is showed in Table 3 for all the studied steels, as expected and reported in the literature (researches cited in the introduction of this article) for several materials.

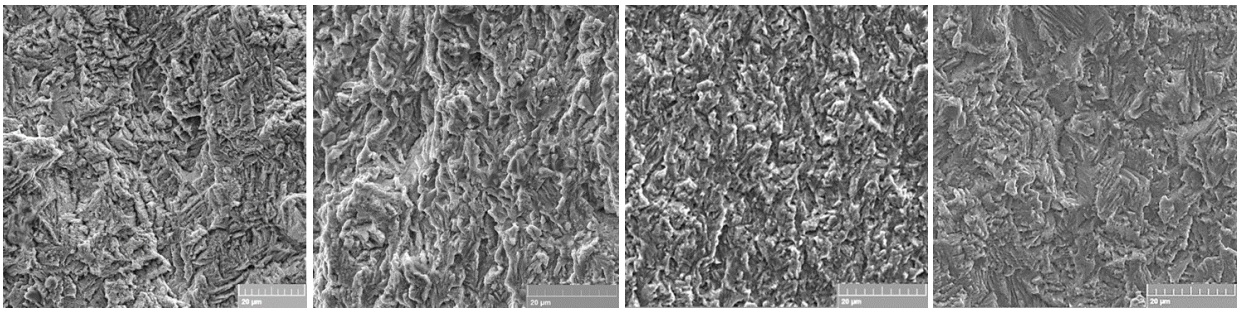

(a) S1 steel (b) S2 steel (c) S3 steel (d) S4 steel

Figure 5. Surface fractography, SEM, of fatigue specimens. *da/dN* ≈ 1 x 10^{-7} mm/cycle.

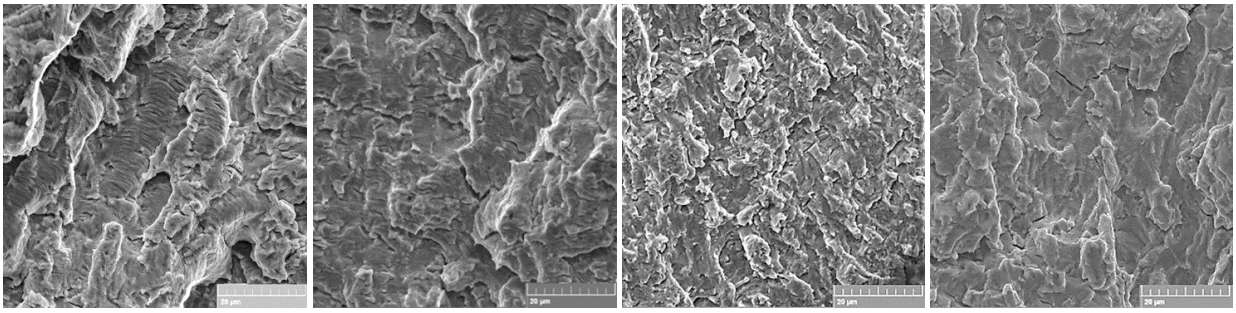

(a) S1 steel (b) S2 steel (c) S3 steel (d) S4 steel

Figure 6. Surface fractography, SEM, of fatigue specimens. $da/dN \approx 1 \times 10^{-5}$ mm/cycle.

Table 3. Effect of *R*-ratio on the fatigue threshold (ΔK_{th}) for the studied steels.

Steel	R = 0.03	R = 0.1	R = 0.4	R = 0.5	R = 0.7
S1	6.74	6.19	6.29	-	3.97
S2	5.76	6.57	-	5.01	4.35
S3	6.00	8.00	-	5.01	3.95
S4	7.73	7.03	6.94	-	5.67

For the application of the Zhu's methodology (2015), it was considered $R_c = 0.7$. The values of the coefficients of Eq. 3 and Eq. 4 for each steel are presented in Table 4. It is important to note that some correlation coefficients (R^2) found in the adjustments for Eq. 3 and Eq. 4 are low, indicating error in the used approximations. According to Eq. 1 and Eq. 2, the predicted *da/dN versus ΔK* relationship is compared with the experimental data, as shown in Fig. 7 for all steels. It can be observed that the predicted curves present the same tendency of the experimental results, but with an error of up to 24%. This indicates the prediction of FCG behavior from R of 0.7 to 0.03 is possible based on the proposed merged approach, but needs improvements. The fatigue thresholds ΔK_{th} are also predicted when the value of $\Delta K_{th(0.7)}$ in Eq. 2 is chosen at the *da/dN* of 1×10^{-7} mm/cyc, and shown in Fig.8, for all steels and the results obtained by Zhu and co-authors (2015). The fatigue thresholds from experiments are similar to those predicted by the model in Eq. 1 and Eq. 2, but also presents error in relation to the experimental results. Another significant problem is that the model predicted the best performance for S4 steel, while S3 steel presented the best experimental behavior.

In order to reduce the errors, the complex mathematical manipulation would require the adoption of a greater range of values for the *R*-ratio, to imply a greater precision in the determination of the A(R) and B(R) functions, Eq.3 and Eq.4. Another aspect to consider is the choice of a more representative equation between *da/dN* and *ΔK* for the threshold region than the Paris equation.

Table 4: Values of the parameters of Equations 3 and 4 for all studied steels. R^2 = correlation coefficient.

Steel	*a*	*b*	*c*	R^2	*d*	*e*	R^2
S1	3.09	-1.16	0.33	0.99	-0.79	0.62	0.85
S2	-3.77	3.45	0.58	0.44	-0.33	0.08	0.13
S3	2.03	-0.33	0.27	0.99	-1.01	0.64	0.95
S4	0.68	0.44	0.46	0.84	-0.51	0.36	0.91

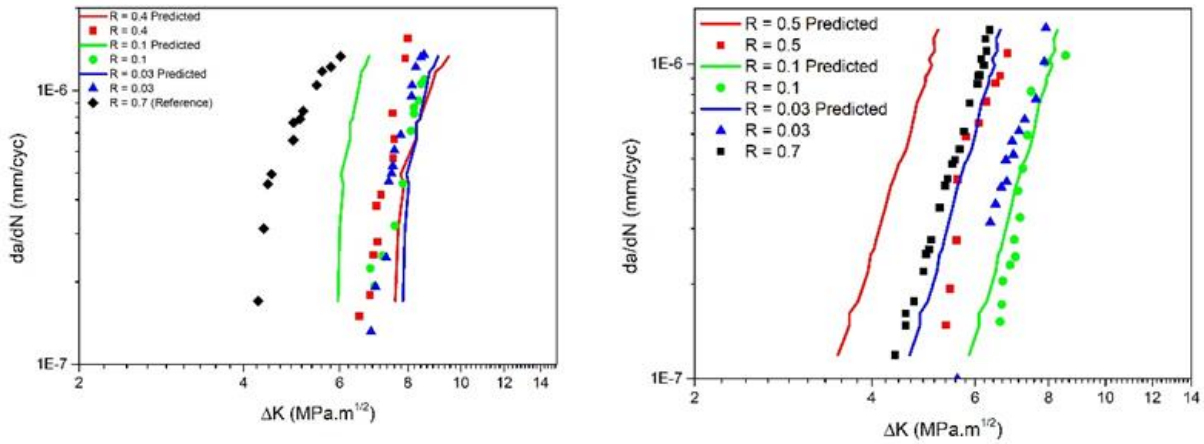

(a) (b)

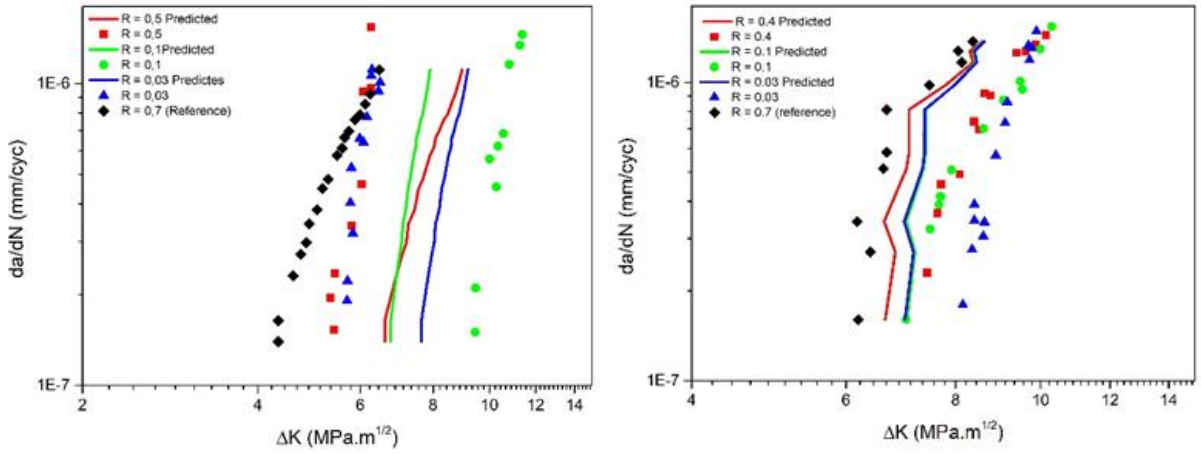

(c) (d)

Figure 7. Comparison of experimental and predicted *da/dN x ΔK* relationships in the near-threshold regime for (a) S1steel; (b) S2 steel; (c) S3 steel; (d) S4 steel.

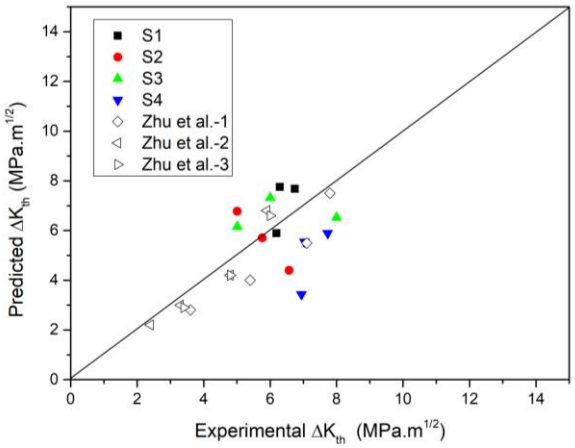

Figure 8. Predicted versus experimental fatigue thresholds for the studied steels and results from Zhu *et al.* (2013, 2015) in a variety of Cr–Mo–V steels.

4. CONCLUSIONS

The model proposed by Zhu and co-authors seems to be a promising methodology for predicting the fatigue crack growth of materials, especially in the threshold region. One advantage of the model is the consideration of the effect of crack closure on fatigue behavior, without the need for its experimental calculation. However, it is a method that requires a relatively complex mathematical manipulation, which must be performed with care. To improve the accuracy, the method should consider a relatively large range of *R* and adopt as a starting point a more precise relation between *da/dN* and *ΔK* than the Paris equation in the threshold region.

5. ACKNOWLEDGEMENTS

T.F.M. would like to acknowledge CNPq for financial support.

6. REFERENCES

Al-Rubaie, K.S., Barroso, E.K.L. and Godefroid, L.B., 2008. "Statistical modeling of fatigue crack growth rate in pre-strained 7475-T7351 aluminium alloy". *Materials Science and Engineering A*, Vol. 486, pp. 585-595.

ASTM E647-15, 2016. *Standard Test Method for Measurement of Fatigue Crack Growth Rates*. American Society for Testing and Materials.

Boyce, B.L. and Ritchie, R.O., 2001. "Effect of load ratio and maximum stress intensity on the fatigue threshold in Ti–6Al–4V". *Engineering Fracture Mechanics*, Vol. 68, pp. 129–147.

Dasarathy, C. and Goodwin, T.J., 1990. "Recent developments in automotive steels", *Metals & Materials*, Vol. 6, pp. 21-28.

De, A.K., Speer, J.G. and Matlock, D.K., 2003. "Color tint-etching of multi-phase steels". *Advanced Materials and Processes*, February, pp. 27-30.

Dubey, S., Soboyejo, A.B.O. and Soboyejo, W.O., 1997. "An investigation of the effects of stress ratio and crack closure on the micromechanisms of fatigue crack growth in Ti–6Al–4V". *Acta Materialia,* Vol. 45, pp. 2777–2787.

Dutta, V.B., Suresh, S. and Ritchie, R.O. 1984. "Fatigue crack propagation in dual-phase steels". *Metallurgical Transactions*. Vol.15(A), pp. 1193-1207.

Elber, W., 1971. "The significance of fatigue crack closure". *Damage Tolerance in Aircraft Structures – ASTM STP 486*. American Society for Testing and Materials, pp. 230-242.

El-Shabasy, A.B. and Lewandowski, J.J., 2004. "Effects of load ratio R and temperature on fatigue crack growth of fully pearlitic eutectoid steel". *International Journal of Fatigue*, Vol. 26, pp. 305-309.

Godefroid, L.B., Andrade, M.S., Machado, F.A. and Horta, W.S. 2011. "Effect of prestrain and bake hardening heat treatment on fracture toughness and fatigue crack growth resistance of two dual-phase steels". In: Proceedings of the Materials Science And Technology Conference; Oct 16-20; Columbus, OH, USA.

Godefroid, L.B., Moreira, L.P., Vilela, T.C.G., Faria, G.L., Candido, L.C. and Pinto, E.S., 2019. "Effect of chemical composition and microstructure on the fatigue crack growth resistance of pearlitic steels for railroad application". *International Journal of Fatigue*, Vol. 120, pp. 241-253.

Gritti, J.A., Melo, T.M.F., Machado, F.A., Silva, A.P.F.S., Guimarães, C.R., Cândido, L.C. and Godefroid, L.B. 2014. "Propagação e fechamento de trinca de fadiga em dois aços bifásicos pré-deformados e com tratamento de bake hardening". *Tecnologia em Metalurgia e Materiais*. Vol. 2, pp. 71–75.

Gutz, A.E., Machado, F.A., Gritti, J.A., Melo, T.M.F., Cândido, L.C. and Godefroid, L.B. 2010. "Tenacidade à fratura e resistência ao crescimento de trinca por fadiga de um aço bifásico da classe de 780MPa de resistência". In: Proceedings of the 65° Congresso Anual da ABM; Rio de Janeiro, BR.

Jones, R., Molent, L. and Walker, K., 2012. "Fatigue crack growth in a diverse range of materials". *International Journal of Fatigue*, Vol. 40, pp. 43-50.

Keeler, S. and Kimchi, M., 2017. "Advanced High-Strength Steels Application Guidelines". *WordAutoSteel*, Vol. 5.

Krauss, G., 2005. *Steels: Processing, structure and performance*. ASM International.

Liaw, P.K., Leax, T.R. and Logsdon, W.A., 1983. "Near-threshold fatigue crack growth behavior in metals". *Acta Metallurgica*, Vol. 31, pp. 1581-1587.

Minakawa, K., Matsuo, Y. and Mcevily, A.J. 1982 "The influence of a duplex microstructure in steels on fatigue crack growth in the near-threshold region". *Metallurgical Transactions.* Vol.13(A), pp. 439-445.

Ramage, R.M., Jata, K.V., Shiflet, G.J. and Starke, E.A. 1987. "The effect of phase continuity on the fatigue and crack closure behavior of a dual-phase steel". *Metallurgical Transactions*. Vol. 18(A), pp. 1291-1298.

Ritchie, R.O., 1979. "Near-threshold fatigue-crack propagation in steels". *International Metallurgical Reviews*, Vol. 24, pp. 205–30.

Roy, A.K., Pal, J. and Hasan, M.H., 2010. "Temperature and load ratio effects on crack-growth behavior of austenitic superalloys". *Journal of Engineering Materials and Technology*, Vol. 132(1), pp. 1-7.

Sarwar, M. and Priestner, R. 1999. "Fatigue crack propagation behaviour in dual-phase steel". *Journal of Materials Engineering and Performance.* Vol. 8, pp. 245-251.

Sun, L., Li, S., Zang, Q. and Wang, Z. 1995. "Dependence of fatigue crack closure behaviour on volume fraction of martensite in dual-phase steels". *Scripta Metallurgica*. Vol. 32, pp. 517-521.

Vasudevan, A.K., Sadananda, K. and Louat, N., 1994. "A review of crack closure, fatigue crack threshold and related phenomena". *Materials Science and Engineering A*, Vol. 188, pp. 1-22.

Zhihong, Z., Yuefeng, G., Osada, T., Yong, Y., Chuanyong, C., Yokokawa, T., Tetsui, T. and Harada, H., 2011. "Fatigue crack growth characteristics of a new Ni–Co-base superalloy TMW-4M3: effects of temperature and load ratio". *Journal of Materials Science*, Vol. 46, pp. 7573–7581.

Zhu, M.L., Xuan, F.Z. and Tu, S.T., 2013. . "Interpreting load ratio dependence of near-threshold fatigue crack growth by a new crack closure model". *International Journal of Pressure Vessels and Piping*, Vol. 110, pp. 9-13.

Zhu, M.L., Xuan, F.Z. and Tu, S.T., 2015. "Effect of load ratio on fatigue crack growth in the near-threshold regime: a literature review, and a combined crack closure and driving force approach". *Engineering Fracture Mechanics*, Vol. 141, pp. 55-77.

7. RESPONSIBILITY NOTICE

The authors are the only responsible for the printed material included in this paper.